East European Journal of Physics. 1. 350-356 (2025)
DOI:10.26565/2312-4334-2025-1-43 ISSN 2312-4334

ULTRASOUND DOPPLER SYSTEM'S RESOLUTION USING COHERENT PLANE-WAVE COMPOUNDING TECHNIQUE

Evgen A. Barannik, Mykhailo O. Hrytsenko*
Department of Medical Physics and Biomedical Nanotechnologies, V.N. Karazin Kharkiv National University
4 Svobody Sq., 61022, Kharkiv, Ukraine
**Corresponding Author: mykhailo.hrytsenko@student.karazin.ua*
Received November 14, 2024; revised January 5, accepted February 12, 2025

Among modern ultrasound technologies for medical diagnostics, a special place is held by the technology of compounding plane waves with different propagation directions, which form synthesized images. In this work, based on the previously developed theory of Doppler response formation, the resolution of a system that uses plane wave compounding is investigated. In this case, small nonlinear components in the angle of inclination of the wave vectors of different plane waves were taken into account for the phase of the synthesized response and for the envelope of the radiation pulses. As a result of the study, it was found that the dimensions of the measuring volume in the longitudinal and transverse directions do not change. Taking into account small components leads to a slight change in the shape of the measuring volume, which ceases to be exactly spherical. This is explained by the fact that the resolution is determined not only by the interference of plane waves, but also by the area of their intersection at a certain point in space. The results obtained indicate that neglecting small inclination angles in the envelope is fully justified and allows simplifying the process of obtaining Doppler signal spectra in plane wave compounding technology.
Keywords: *Ultrasound; Doppler spectrum; Plane wave compounding; Sensitivity function; Spatial resolution; Envelope*
PACS: 43.28.Py, 43.35.Yb, 43.60.-c, 87.63.D-, 87.63.dk

INTRODUCTION

Due to the advancement of technology and the significant increase in the capabilities of computer systems, methods of ultrasound diagnostics requiring extensive computations are actively evolving. To achieve high-resolution imaging in every point of the entire analyzed area, synthetic aperture (SA) methods using ultrasound waves with various spatial configurations are increasingly employed compared to traditional imaging methods [1,2]. A distinctive feature of this method is that ultrasound echo signals from each spatial point are coherently accumulated for different wavefront propagation angles. Since the SA method enables focusing in each spatial point and constructing high-frame-rate images, it has found applications in various medical areas, including Doppler imaging [3-6,9], elastography [8], and more. Enhancing and analyzing the quality of the obtained images and integrating these methods into existing ultrasound diagnostic systems are important challenges [9-12].

Technologies based on this method are advancing rapidly, particularly ultrasound probing using plane ultrasonic waves [13,14,9] with various propagation directions [15,16,9]. For example, through the technology of plane-wave compounding (PWC), improvements in Doppler evaluations, especially for slow blood flows, have been achieved compared to conventional methods [4,19-21]. Additionally, experimental studies using this technology have investigated velocity vector estimation [17,18], visualized vessel walls, implemented color and 3D ultrafast Doppler imaging, brain functional imaging, and elasticity visualization using shear waves [22-24,4,5,9].

Each emission of single ultrasonic plane waves produces only low-quality images. However, coherent accumulation of echo signals from waves propagating at different angles yields high-quality images with frame rates of several kilohertz, increasingly utilized in medicine today [25,26]. PWC simultaneously provides high-quality B-mode images [27-30] and a continuous data stream for Doppler analysis methods [31-34,22].

Various approaches to improving PWC resolution are actively being developed, including novel adaptive compounding techniques [35], the use of artificial intelligence [36,37], beamforming strategies [38,39], motion correction schemes based on multi-angle vector Doppler velocity estimates [40], employing multiple transducer arrays for plane-wave compounding [41], multiperspective imaging with curved arrays [42], and methods for increasing frame rates [43], among others.

Improving the quality of ultrasound and Doppler diagnostics using coherent plane-wave compounding technology remains a pressing issue. Based on the original developed theory of Doppler response formation [44-46], theoretical resolution estimates for systems applying PWC were previously obtained [47]. These studies considered only linear phase components of plane waves with small deviations in wave vectors. The aim of this work is to investigate the resolution of ultrasound systems utilizing PWC, accounting for nonlinear components in both the response signal phase and the envelopes of transmitted plane-wave pulses.

Cite as: E.A. Barannik, M.O. Hrytsenko, East Eur. J. Phys. 1, 350 (2025), https://doi.org/10.26565/2312-4334-2025-1-43

THEORETICAL MODEL

Previously [46-48], in theoretical studies of the spectral characteristics of ultrasound Doppler response signals in systems utilizing PWC, the complex amplitude of the transmitted field $G_t(\vec{r},t)$ and the complex sensitivity function of the receiver to scattered waves $G_r(\vec{r},t)$ were used. Physically, these functions describe the ultrasound fields of transmission and receiving, taking into account their deviation from a plane wave with a constant wave vector $\vec{k}$, aligned with the x' axis of the ultrasonic fields shown in Fig. 1.

This approach is particularly convenient when describing traditional ultrasound diagnostic systems [44,45], as they utilize stationary ultrasound fields. The time dependence of these functions arises specifically with PWC, where the probing direction changes over time according to a defined wave vector $\vec{k}(t)$. In this case, it is more convenient to use an approach based on the direct wave fields of transmission $P_t'(\vec{r},t)$ and receiving $P_r'(\vec{r},t)$, represented as plane waves with the wave vector $\vec{k}(t)$. Here, the vector $\vec{k}$ represents the time-averaged wave vector directed along the x' axis.

From this point forward, we assume that both the acquisition of ultrasound Doppler response signals and the emission with plane wavefronts occur at the same angle Φ, as illustrated in Fig. 1. Thus, the resulting transmission-receiving field can be expressed as follows

$$P(\vec{r},t) = G_t(\vec{r},t)G_r(\vec{r},t)e^{2i\vec{k}\vec{r}}b\left(T_1-\frac{2x''}{c_0}\right)g(z) = P_t(\vec{r},t)P_r(\vec{r},t)b\left(T_1-\frac{2x''}{c_0}\right)g(z) =$$
$$P_tP_re^{2i\vec{k}(t)\vec{r}}b\left(T_1-\frac{2x''}{c_0}\right)g(z) \equiv P_0e^{2i\vec{k}(t)\vec{r}}b\left(T_1-\frac{2x''}{c_0}\right)g(z). \quad (1)$$

Where P_t and P_r are, respectively, the real amplitudes of the transmitted and received plane waves; $b\left(T_1-\frac{2x''}{c_0}\right)$ is the envelope of the ultrasonic transmitted pulses; and $g(z)$ represents the field distribution along the z axis.

The pulse envelope describes their spatial length in the direction $x'' = x''(x',y')$, i.e., in the direction of the emission and receiving of plane waves for a given wave vector $\vec{k}(t)$ and corresponding angle Φ. As shown in Fig. 1, the distance l_0'' to a given target point, i.e., the probing depth, is determined by the strobing time delay T_1.

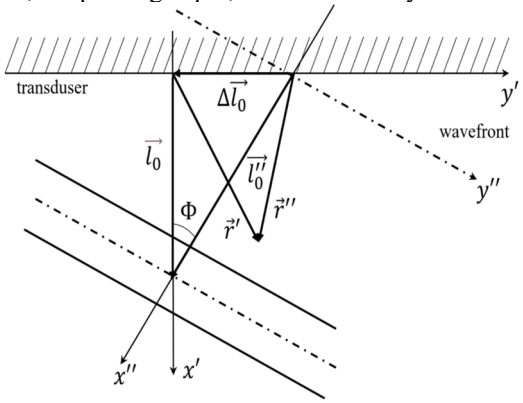

Figure 1. Coordinate system (x',y') associated with the ultrasonic transducer and coordinate system (x'',y''), where the x''axis is directed along the propagation direction of the plane wavefront

According to the continuous model of ultrasound wave scattering on density inhomogeneities $\rho(\vec{r},t)$ and compressibility $\tilde{\beta}(\vec{r},t)$ the ultrasound Doppler response signal can now be expressed in a simplified form as:

$$e_d(t) = k^2\int_R P_p'(\vec{r},t)\left\{\tilde{\beta}(\vec{r},t)-\rho(\vec{r},t)\right\}d\vec{r}. \quad (2)$$

The power spectral density of the response signal is determined through the temporal and spatial Fourier transform of the autocorrelation function of the response signal (2):

$$R(\tau) = k^4\iint_R \overline{P(\vec{r}_1,t_1)P^*(\vec{r}_0,t_0)}\,C\left(\vec{r}_1-\vec{r}_0,\tau\right)d\vec{r}_0d\vec{r}_1,$$

The overline indicates averaging over the initial moment of time t_0, and $C\left(\vec{r}_1-\vec{r}_0,\tau\right)$ is the correlation function of fluctuations of density and compressibility inhomogeneities, whichdepends only on the difference in coordinates and the time difference $\tau = t_1 - t_0$ for any type of scatterer motion after averaging over the statistical ensemble [48].

The Doppler spectrum is derived in full analogy with the method in [48] and, in the absence of signal accumulation from different directions, can be represented as:

$$S(\omega_p) = \frac{k^4}{(2\pi)^3}\sum_{\omega_j}\int d\vec{q}\,C(\vec{q},\omega_p-\omega_j)\left|P(\vec{q},\omega_j)\right|^2.$$

where $C(\vec{q},\omega_p-\omega_j)$ and $P(\vec{q},\omega_j)$ are the Fourier transforms of the fluctuation correlator and the transmission-receiving field, respectively. When compounding responses from different plane waves, which is a widely accepted algorithm in all variations of the synthetic aperture method, the Doppler response takes the form:

$$S(\omega_p)=\frac{k^4}{(2\pi)^3}\int d\vec{q}C(\vec{q},\omega_p)|P(\vec{q},0)|^2. \tag{3}$$

Here, $\omega_p=\frac{2\pi}{T}p$ is the discrete frequency of the Fourier transform of the function $P(\vec{r},t)$, which is periodically extended with a period T. The value T represents the data acquisition period of response signals required for wave compounding.

RESULTS

Directly from expression (3), it follows that in the case of compounding plane waves, the quantity $P(\vec{r},0)$ serves as the transmission-receiving field. Furthermore, following [48], the envelope of the emitted pulses will be chosen in the form of a Gaussian function. In this approximation, the transmission-receiving field (1) can be written as:

$$P(\vec{r},t)=P_0e^{-2ik\left((l_0-x')cos\Phi+y'sin\Phi\right)}e^{-\frac{2\left((l_0-x')cos\Phi+y'sin\Phi\right)^2}{a^2}}g(z), \tag{4}$$

where $2a$ is the spatial length of the pulses along the x''axis at the e^{-1} level. In formula (4), the relationship between the coordinate system (x',y') and the coordinate systems (x'',y'') and (x,y) is taken into account. Assuming the angles $\Phi(t)=\Omega t$ are small for all plane waves, in the expansion of the transmission-receiving field in terms of Φ, we will retain small terms, including quadratic ones. To estimate the Fourier transforms in this approximation, we will apply a Gaussian weighting window in time, which allows extending the integration limits to infinity:

$$P(\vec{r},\omega_j)=P_0g(z)T^{-1}e^{-\frac{2(l_0-x')^2}{a^2}}\int_{-\frac{T}{2}}^{\frac{T}{2}}e^{e^{-2ik\left(\frac{-\Omega^2t^2}{2}(x'-l_0)+\Omega ty'\right)+i\omega_jt}e^{-\frac{2\left(y'^2\Omega^2t^2+2(l_0-x')y'\Omega t-(l_0-x')^2\Omega^2t^2\right)}{a^2}}}dt\cong$$

$$\cong P_0g(z)T^{-1}e^{-\frac{2(l_0-x')^2}{a^2}}\int_{-\infty}^{+\infty}e^{-2ik\left(\frac{-\Omega^2t^2}{2}(x'-l_0)+\Omega ty'\right)+i\omega_jt}e^{-\frac{2\left(y'^2\Omega^2t^2+2(l_0-x')y'\Omega t-(l_0-x')^2\Omega^2t^2\right)}{a^2}}e^{-\frac{t^2}{T_W^2}}dt, \tag{5}$$

where the parameter $T_W\sim T$ in practice describes the effective length of the response signal obtained when applying signal compounding from plane wave responses.

The asymptotic estimate of the integral in (5) can be obtained using the saddle point method, which gives:

$$P(\vec{r},\omega_j)=P_0g(z)T^{-1}e^{-\frac{2(l_0-x')^2}{a^2}-2ik(x'-l_0)}\times$$

$$\times\sqrt{\frac{\pi}{-ik\Omega^2(x'-l_0)+\frac{2y'^2\Omega^2}{a^2}-\frac{2(l_0-x')^2\Omega^2}{a^2}+\frac{1}{T_W^2}}}e^{\frac{\left(2ik\Omega y'-i\omega_j+\frac{4(l_0-x')y'\Omega}{a^2}\right)^2}{4\left(-ik\Omega^2(x'-l_0)+\frac{2y'^2\Omega^2}{a^2}-\frac{2(l_0-x')^2\Omega^2}{a^2}+\frac{1}{T_W^2}\right)}} \tag{6}$$

The small parameter in formulas (5) and (6) is represented by the value $\Omega T_W\sim\Phi_{max}\ll 1$, where Φ_{max} is the maximum angle of inclination of the wave vector $\vec{k}(t)$ from its mean value $\vec{k}$. It is easy to see that for $\omega_j=0$, the numerator of the exponent in the second exponential term in (6) is of the second order of smallness. Therefore, in the denominator of this exponent the small terms can be neglected:

$$P(\vec{r},0)=P_0g(z)T^{-1}e^{-\frac{2(l_0-x')^2}{a^2}-2ik(x'-l_0)}\times$$

$$\times\sqrt{\frac{\pi}{-ik\Omega^2(x'-l_0)+\frac{2y'^2\Omega^2}{a^2}-\frac{2(l_0-x')^2\Omega^2}{a^2}+\frac{1}{T_W^2}}}e^{(\Omega T_Wy')^2\left(ik+\frac{2(l_0-x')}{a^2}\right)^2}.$$

Furthermore, the primary dependence of $P(\vec{r},0)$ on the coordinates is evidently described by exponential factors, which allows us to neglect small quadratic terms in the denominator of the fraction under the square root. As a result, we obtain:

$$P(\vec{r},0)=P_0T^{-1}\sqrt{\pi T_W^2}g(z)e^{-\frac{2(l_0-x')^2}{a^2}-2ik(x'-l_0)}e^{(\Omega T_Wy')^2\left(ik+\frac{2(l_0-x')}{a^2}\right)^2}.$$

Finally, for the modulus of this quantity, we have:

$$|P(\vec{r},0)| = P_0 g(z) e^{-\frac{2(l_0-x')^2}{a^2}} T^{-1} \sqrt{\pi T_W^2} e^{-(\Omega T_W y')^2 \left(k^2 - \frac{4(l_0-x')^2}{a^4}\right)} \tag{7}$$

The parameters in synthetic aperture technologies should be chosen such that the resolution along the y'axis is no worse than in other directions. Therefore, we will assume that the equality $T_W\Omega = \sqrt{2}(ka)^{-1}$holds. Taking this into account, formula (7) takes its final form:

$$|P(\vec{r},0)| = P_0 T^{-1} \sqrt{\pi T_W^2} e^{-\frac{2(l_0-x')^2 - 2z^2}{a^2}} e^{-\frac{2y'^2}{a^2}\left(1 - \frac{4(l_0-x')^2}{k^2 a^4}\right)} g(z). \tag{8}$$

DISCUSSION

The size and shape of the measuring volume are directly described by formula (8), from which, in particular, the equation for the boundary of the measuring volume at the e^{-1} level follows:

$$\frac{2(l_0-x')^2}{a^2} + \frac{2y'^2}{a^2} - \frac{8(l_0-x')^2 y'^2}{a^6 k^2} = 1\,. \tag{9}$$

From this, we find:

$$l_0 - x' = \pm \frac{a^2 k}{2} \sqrt{\frac{\frac{a^2}{2} - y'^2}{\frac{a^4 k^2}{4} - y'^2}}. \tag{10}$$

This function has zeros at $y' = \pm a/\sqrt{2}$, which describe the boundaries of the measuring volume along the y'axis at $x' = l_0$.It is easy to see that for $y' = 0$, equation (10) gives the same boundary values for the x'axis: $x' = l_0 \pm a/\sqrt{2}$. The obtained solution is valid in the case where the inequality holds:

$$\frac{a^2}{2} < \frac{a^4 k^2}{4}, \tag{11}$$

in which the denominator of the fraction under the square root remains positive as the numerator approaches zero. Formally, equation (10) has additional real solutions in the region where both the numerator and the denominator become negative. However, such solutions are physically invalid, as the measuring volume would acquire additional infinite boundaries, as illustrated in Fig. 2.

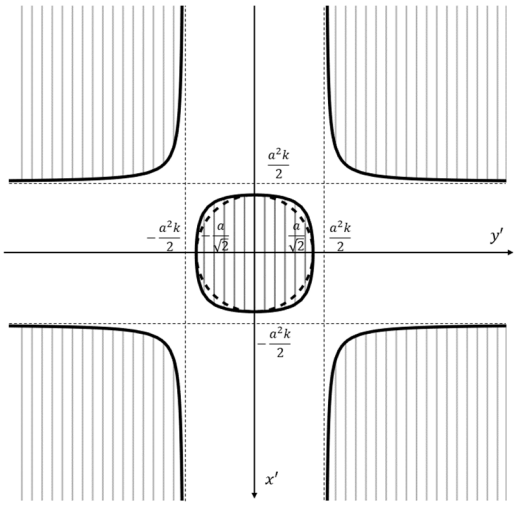

Figure 2. The measuring volume at the center (horizontally shaded) and its boundaries, which are symmetric with respect to x' and y', along with additional non-physical solutions—branches (vertically shaded) and their asymptotes.

The zeros of the denominator in (10) define the asymptotes of these non-physical regions. Without accounting for the dependence of the pulse envelope on small terms, i.e., without the third term on the left-hand side of equation (9), the measuring volume in the (x',y') plane represents a circle with a radius of $a/\sqrt{2}$, shown in Fig. 2 as a horizontal dashed line. This shape is determined by the chosen value of Ω. Considering the dependence of the pulse envelope on

small linear and quadratic terms results in the resolution along the y' and x' axes remaining unchanged, but the shape of the measuring volume changes along with an increase in its area, as shown in Fig. 2 by the horizontal dashed line. This phenomenon is related to the fact that resolution is determined not only by the interference of responses from plane waves but also by the shape of the region of their intersection around the point l_0. When the inverse inequality to (11) is satisfied, an increase in the value of y'^2 causes the denominator of the fraction in (10) to first reach zero. Such a solution is also non-physical because, in this case, the measuring volume has no boundaries, as illustrated in Fig. 3.

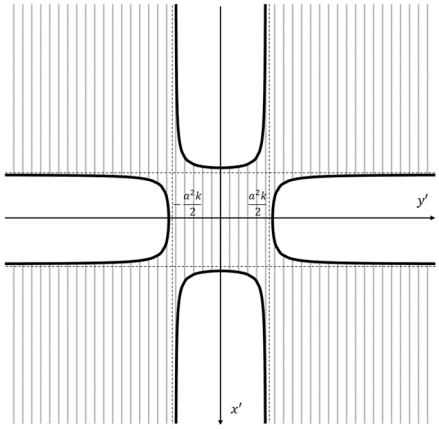

Figure 3. Non-physical infinite measurement volume and its symmetric asymptotes in the case of the inverse of inequality (11) being satisfied

The inequality (11) can be rewritten as $a > \lambda/\sqrt{2}\pi$, which holds well for real ultrasound systems. Specifically, for a frequency of 3.5 MHz, the wavelength is 0.42 mm and the characteristic value of a is 1 mm. This condition becomes even more intuitive from a physical perspective when expressed in terms of the maximum angle of inclination $\Phi_{max} \cong T_W\Omega < 1$. In fact, this is the condition for the smallness of the maximum angle of inclination, for which the obtained solutions are still valid. In the considered approximation, when $\Phi_{max} \cong T_W\Omega = 1$, the measurement volume in the (x', y')plane becomes a square.

CONCLUSIONS

In this work, based on the continuum model of ultrasound wave scattering on inhomogeneities in the medium, the resolution of the PWC system is analyzed. The consideration is carried out taking into account the linear and quadratic terms in the expansion of the small deviations of the wave vector of the current viewpoint from the wave vector of a plane wave without inclination. The condition of smallness of the inclination angles of the plane waves ensures the physicality and correctness of the obtained solutions. The results show that accounting for linear and quadratic angle Φ deviations in the directions of wave transmission and receiving only leads to changes in the shape and volume of the measured volume, which, without accounting for small components, has a spherical shape. At the same time, the dimensions of the measurement volume in the longitudinal and transverse directions do not change.

The noted change in the shape of the measurement volume for realistic values of the maximum inclination angle Φ_{max} is not significant. As is known, the size of the measured volume only affects the time of flight of scatterers through it, which also does not change significantly. This means that the contribution to the Doppler spectrum width, determined by the flight time, cannot change significantly either. Therefore, it can be concluded that when evaluating the spectral characteristics of the ultrasound Doppler response signals, it is quite justified to neglect the dependence of the envelope of the plane wave pulses on the inclination angles if they are small. This circumstance opens the possibility for simplifying spectral Doppler estimates.

ORCID

Evgen A. Barannik, https://orcid.org/0000-0002-3962-9960; **Mykhailo O. Hrytsenko,** https://orcid.org/0009-0002-5670-5686

REFERENCES

[1] I. Trots, A. Nowicki, M. Lewandowski, and Y. Tasinkevych, *Synthetic Aperture Method in Ultrasound Imaging*, (IntechOpen, London, UK, 2011). http://dx.doi.org/10.5772/15986

[2] M.H. Pedersen, K.L. Gammelmark, and J.A. Jensen, Ultrasound Med. Biol. **33**(1), 37-47 (2007). https://doi.org/10.1016/j.ultrasmedbio.2006.07.041

[3] J. Bercoff, G. Montaldo, T. Loupas, D. Savery, F. Meziere, M. Fink, and M. Tanter, IEEE Trans. Ultrason. Ferroelec. Freq. Contr. **58**(1), 134 (2011). https://doi.org/10.1109/TUFFC.2011.1780

[4] J. Provost, C. Papadacci, C. Demene, J. Gennisson, M. Tanter, and M. Pernot, IEEE Trans. Ultrason. Ferroelec. Freq. Contr. **62**(8), 1467 (2015). https://doi.org/10.1109/TUFFC.2015.007032

[5] J. Udesen, F. Gran, K.L. Hansen, J.A. Jensen, C. Thomsen and M.B. Nielsen, IEEE Trans. Ultrason. Ferroelec. Freq. Contr. **55**(8), 1729 (2008). https://doi.org/10.1109/TUFFC.2008.858

[6] B. Osmanski, M. Pernot, G. Montaldo, A. Bel, E. Messas, and M. Tanter, IEEE Trans. Med. Imag. **31**(8), 1661 (2012). http://doi.org/10.1109/TMI.2012.2203316
[7] C. Papadacci, M. Pernot, M. Couade, M. Fink and M. Tanter, IEEE Trans. Ultrason. Ferroelec. Freq. Contr. **61**(2), 288 (2014). https://doi.org/10.1109/TUFFC.2014.6722614
[8] G. Montaldo, M. Tanter, J. Bercoff, N. Benech, and M. Fink, IEEE Trans. Ultrason. Ferroelectr. Freq. Contr. **56**(3), 489 (2009). https://doi.org/10.1109/TUFFC.2009.1067
[9] J. Jensen, M.B. Stuart, and J.A. Jensen, IEEE Trans. Ultrason. Ferroelec. Freq. Contr. **63**(11), 1922 (2016). https://doi.org/10.1109/TUFFC.2016.2591980
[10] B. Denarieetal, IEEE Trans. Med. Imaging, **32**(7), 1265 (2013). https://doi.org/10.1109/TMI.2013.2255310
[11] R. Moshavegh, J. Jensen, C.A. Villagómez-Hoyos, M.B. Stuart, M.C. Hemmsenand, and J.A. Jensen, in: *Proceedings of SPIE Medical Imaging*, (SanDiego, California, United States, 2016), pp. 97900Z-97900Z-9. https://doi.org/10.1117/12.2216506
[12] J.-l. Gennisson, et al., IEEE Trans. Ultrason. Ferroelec. Freq. Contr. **62**(6), 1059 (2015). https://doi.org/10.1109/TUFFC.2014.006936
[13] J.A. Jensen, S.I. Nikolov, K.L. Gammelmarkand, and M.H. Pedersen, Ultrasonics, **44**(1), e5 (2006). https://doi.org/10.1016/j.ultras.2006.07.017
[14] M. Tanter, J. Bercoff, L. Sandrin, and M. Fink, IEEE Trans. Ultrason. Ferroelectr. Freq. Contr. **49**(10), 1363 (2002). https://doi.org/10.1109/TUFFC.2002.1041078
[15] J.Y. Lu, IEEE Trans. Ultrason., Ferroelec. Freq. Contr. **44**(4), 839 (1997). https://doi.org/10.1109/58.655200
[16] S. Ricci, L. Bassi and P. Tortoli, IEEE Trans. Ultrason. Ferroelec. Freq. Contr. **61**(2), 314 (2014). https://doi.org/10.1109/TUFFC.2014.6722616
[17] N. Oddershedeand J.A. Jensen, IEEE Trans. Ultrason. Ferroelec. Freq. Contr. **54**(9), 1811 (2007). https://doi.org/10.1109/TUFFC.2007.465
[18] Y. L, Li, D. Hyun, L. Abou-Elkacem, J. K. Willmann, J.J. Dahl, IEEE Trans. Ultrason. Ferroelec. Freq. Contr. **63**(11), 1878 (2016), https://doi.org/10.1109/TUFFC.2016.2616112
[19] Y.L. Li, J.J. Dahl, IEEE Trans. Ultrason. Ferroelec. Freq. Contr. **62**(6), 1022 (2015). https://doi.org/10.1109/TUFFC.2014.006793
[20] I. K. Ekroll, A. Swillens, P. Segers, T. Dahl, H. Torp and L. Lovstakken, IEEE Trans. Ultrason. Ferroelec. Freq. Contr. 60(4), 727 (2013). https://doi.org/10.1109/TUFFC.2013.2621
[21] S. Salles, H. Liebgott, O. Basset, C. Cachard, D. Vray, and R. Lavarello, IEEE Trans. Ultrason. Ferroelectr. Freq. Control, **61**, 1824–1834 (2014). https://doi.org/10.1109/TUFFC.2014.006543
[22] C.-C. Shen, and and C.-L. Huang, Sensors, **24**, 262 (2024). https://doi.org/10.3390/s24010262
[23] J. Viti, H.J. Vos, N.D. Jong, F. Guidi, and P. Tortoli, "Contrast detection efficacy for plane vs. focused wave transmission," in: *2014 IEEE International Ultrasonics Symposium*, (Chicago, 2014), pp. 1750–1753.
[24] J. Bercoff, "Ultrafast ultrasound imaging," in: *Ultrasound Imaging-Medical applications*, edited by I.V. Minin, and O.V. Minin, pp. 3-24, (2011). https://doi/org/10.5772/19729
[25] C. Demené et al., "Spatiotemporal clutter filtering of ultrafast ultrasound data highly increases Doppler and fUltrasound sensitivity," IEEE transactions on medical imaging, vol. 34, no. 11, pp. 2271-2285, 2015.
[26] S. Salles, F. Varray, Y. Bénane and O. Basset, 2016 IEEE International Ultrasonics Symposium (IUS), 2016, pp. 1-4, https://doi.org/10.1109/ULTSYM.2016.7728751
[27] C. Zheng, Q. Zha, L. Zhang and H. Peng, IEEE Access 6, 495 (2018), https://doi.org/10.1109/ACCESS.2017.2768387
[28] Y.M. Benane et al., 2017 IEEE International Ultrasonics Symposium (IUS), 2017, pp. 1-4, https://doi.org/10.1109/ULTSYM.2017.8091880
[29] X. Yan, Y. Qi, Y. Wang, Y. Wang, Sensors 21, 394 (2021), https://doi.org/10.3390/s21020394
[30] C. Golfetto, I. K. Ekroll, H. Torp, L. Løvstakken and J. Avdal, IEEE Trans. Ultrason. Ferroelec. Freq. Contr. 68(4), 1105 (2021), https://doi.org/10.1109/TUFFC.2020.3033719
[31] C.-C. Shen, Y.-C. Chu, Sensors 21, 4856 (2021), https://doi.org/10.3390/s21144856
[32] J. Baranger, B. Arnal, F. Perren, O. Baud, M. Tanter, and C. Demené, IEEE transactions on medical imaging, 37(7), 1574 (2018). https://doi.org/10.1109/TMI.2018.2789499
[33] A. Daae, M. Wigen, M. Halvorsrød, L. Løvstakken, A. Støylen, S. Fadnes, Ultrasound i Medicine & Biology, **49**(9), 1970 (2023), https://doi.org/10.1016/j.ultrasmedbio.2023.04.019
[34] M. Hashemseresht, S. Afrakhteh, and H. Behnam, Biomedical Signal Processing and Control, **73**, 103446 (2022). https://doi.org/10.1016/j.bspc.2021.103446
[35] K. Miura, H. Shidara, T. Ishii, K. Ito, T. Aoki, Y. Saijo, and J. Ohmiya, Ultrasonics, **145**, 107479 (2025). https://doi.org/10.1016/j.ultras.2024.107479
[36] N. Chennakeshava, B. Luijten, O. Drori, M. Mischi, Y.C. Eldarand and R.J.G. van Sloun, "High ResolutionPlane Wave CompoundingThrough Deep Proximal Learning," in: *2020 IEEE International UltrasonicsSymposium (IUS)*, (Las Vegas, USA, 2020), pp. 1-4, https://doi.org/10.1109/IUS46767.2020.9251399
[37] J. Zhao, Y. Wang, X. Zeng, J. Yu, B.Y.S. Yiu, and A.C.H. Yu, Ferroelectrics, and Frequency Control, **62**(8), 1440 (2015). https://doi.org/10.1109/tuffc.2014.006934
[38] Y. Xu, B. Li, J. Luo, X. Liu, and D. Ta, AIP Advances, **14**(6), 065001 (2024). https://doi.org/10.1063/5.0201371
[39] I.K. Ekroll, M.M. Voormolen, O.K.-V. Standal, J.M. Rau, and L. Lovstakken, IEEE Trans. Ultrason. Ferroelec. Freq. Contr. **62**(9), 1634 (2015). https://doi.org/10.1109/TUFFC.2015.007010
[40] J. Foiret, X. Cai, H. Bendjador, *et.al.,* Sci. Rep. **12**, 13386 (2022). https://doi.org/10.1038/s41598-022-16961-2
[41] S. Afrakhteh, and H. Behnam, IEEE Transactions on Ultrasonics, Ferroelectrics, and Frequency Control, **68**(10), 3094 (2021). https://doi.org/10.1109/tuffc.2021.3087504
[42] R. Paridar, and B.M. Asl, Ultrasonics, **135**, 107136 (2023). https://doi.org/10.1016/j.ultras.2023.107136
[43] E.A. Barannik, Ultrasonics, **39**(2), 311 (2001). https://doi.org/10.1016/S0041-624X(01)00059-2

[44] I.V. Skresanova, and E.A. Barannik, Ultrasonics, **52**(5), 676 (2012). https://doi.org/10.1016/j.ultras.2012.01.014
[45] I.V. Sheina, O.B. Kiselov, and E.A. Barannik, East Eur. J. Phys. (4), 5 (2020), https://doi.org/10.26565/2312-4334-2020-4-01
[46] I.V. Sheina, and E.A. Barannik, East European Journal ofPhysics, (1), 116-122. https://doi.org/10.26565/2312-4334-2022-1-16
[47] E.A. Barannik, and O.S. Matchenko, East Eur. J. Phys. **3**(2) 61 (2016). https://doi.org/10.26565/2312-4334-2016-2-08. (in Russian)
[48] E.A. Barannik, and M.O. Hrytsenko, East Eur. J. Phys. (1), 476 (2024). https://doi.org/10.26565/2312-4334-2024-1-52

РОЗДІЛЬНА ЗДАТНІСТЬ УЛЬТРАЗВУКОВОЇ ДОПЛЕРІВСЬКОЇ СИСТЕМИ З ВИКОРИСТАННЯМ ТЕХНОЛОГІЇ КОГЕРЕНТНОГО КОМПАУНДИНГУ ПЛОСКІХ ХВИЛЬ

Євген О. Баранник, Михайло О. Гриценко
Кафедра медичної фізики та біомедичних нанотехнологій, Харківський національний університет ім. В.Н. Каразіна, 61022, пл. Свободи, 4, м. Харків, Україна

Серед сучасних ультразвукових технологій медичної діагностики особливе місце посідає технологія компаудингу пласких хвиль з різними напрямками поширення, які формують синтезовані зображення. В роботі на базі розвинутої раніше теорії формування допплерівського відгуку досліджена роздільна здатність системи, в якій використовується компаудинг пласких хвиль. При цьому для фази синтезованого відгуку і огинаючої імпульсів випромінювання враховувались малі нелінійні складові по куту відхилення хвильових векторів різних пласких хвиль. В результаті дослідження винайдено, що розміри вимірювального об’єму у поздовжньому та поперечному напрямках не змінюються. Урахування малих складових приводить до незначної зміни форми вимірювального об'єму, який перестає бути точно сферичним. Це пояснюється тим, що роздільна здатність визначається не тільки інтерференцією пласких хвиль, але й областю їх перетину у визначеній точці простору. Отримані результати свідчить про те, що нехтування малими кутами відхилення у огинаючій є повністю виправданим і дозволяє спростити процес отримання спектрів допплерівських сигналів в технології компаундинга пласких хвиль.

Ключові слова: *ультразвук; допплерівський спектр; компаундування плоских хвиль; просторова роздільна здатність; огинаюча імпульсів*